J Biomol NMR (2010) 48:203–212
DOI 10.1007/s10858-010-9450-8

ARTICLE

Quantification of protein backbone hydrogen-deuterium exchange rates by solid state NMR spectroscopy

Juan-Miguel Lopez del Amo · Uwe Fink · Bernd Reif

Received: 21 June 2010 / Accepted: 21 September 2010 / Published online: 20 October 2010

Abstract We present the quantification of backbone amide hydrogen-deuterium exchange rates (HDX) for immobilized proteins. The experiments make use of the deuterium isotope effect on the amide nitrogen chemical shift, as well as on proton dilution by deuteration. We find that backbone amides in the microcrystalline α-spectrin SH3 domain exchange rather slowly with the solvent (with exchange rates negligible within the individual ^{15}N–T_1 timescales). We observed chemical exchange for 6 residues with HDX exchange rates in the range from 0.2 to 5 s^{-1}. Backbone amide ^{15}N longitudinal relaxation times that we determined previously are not significantly affected for most residues, yielding no systematic artifacts upon quantification of backbone dynamics (Chevelkov et al. 2008b). Significant exchange was observed for the backbone amides of R21, S36 and K60, as well as for the sidechain amides of N38, N35 and for W41ε. These residues could not be fit in our previous motional analysis, demonstrating that amide proton chemical exchange needs to be considered in the analysis of protein dynamics in the solid-state, in case D_2O is employed as a solvent for sample preparation. Due to the intrinsically long ^{15}N relaxation times in the solid-state, the approach proposed here can expand the range of accessible HDX rates in the intermediate regime that is not accessible so far with exchange quench and MEXICO type experiments.

Keywords MAS solid-state NMR · Hydrogen-deuterium exchange · Relaxation · Perdeuterated proteins · Alpha-spectrin SH3

For submission to the *Journal of Biomolecular NMR*.

J.-M. L. del Amo · U. Fink · B. Reif (✉)
Leibniz-Institut für Molekulare Pharmakologie (FMP), Robert-Rössle Str. 10, 13125 Berlin, Germany
e-mail: reif@tum.de

B. Reif
Technische Universität München (TUM), Lichtenbergstr. 4, 85747 Garching, Germany

B. Reif
Helmholtz-Zentrum München (HMGU), Deutsches Forschungszentrum für Gesundheit und Umwelt, Ingolstädter Landstr. 1, 85764 Neuherberg, Germany

Introduction

The analysis of the backbone HDX rates in a protein has become an important method to obtain direct information on protein structure (Kato et al. 2009; Raschke and Marqusee 1998; Wagner and Wuthrich 1982), stability (Bai et al. 1995; Wong and Heremans 1988; Kuroda et al. 1995), protein-protein interactions (Dyson et al. 2008; Polshakov et al. 2006) and dynamics (Dempsey 2001; Parker and Marqusee 2000). The interrelation between HDX and structure is determined by the participation of the amide group in secondary structure elements, as well as by its surface accessibility. The largest exchange rates are expected for those backbone amides which are unstructured and close to water. On the other hand, the slowest rates are usually observed for strongly hydrogen bonded amides in secondary structure elements in the hydrophobic core of a protein (Truhlar et al. 2006), or for amides which are located in a lipid environment (Halskau et al. 2002; Pinheiro et al. 2000). It is commonly believed, that HDX rates are additionally correlated to backbone dynamics, since opening of the amide hydrogen bond is required in order to expose the hydrogen to the catalytic solvent (Maity

et al. 2003). The relation between dynamics and hydrogen exchange can be represented by (Hvidt and Nielsen 1966)

$$NH_C \underset{k_C}{\overset{k_O}{\rightleftarrows}} NH_O \xrightarrow{k_{ex}} NH_O^* \quad (1)$$

in which the NH populations in the open (solvent exposed) and closed (structurally hydrogen bonded) states are related by the corresponding opening (k_o) and closing (k_c) rate constants. The detailed chemistry underlying hydrogen exchange is still subject of discussion (Dempsey 2001). Nevertheless, the importance of acid and base catalysis is clear (Gregory et al. 1983). Their contribution to the observed exchange rates are represented by the equation

$$k_{ex} = k_a[H^+] + k_b[OH^-] + k_w, \quad (2)$$

where the measured exchange rate constant k_{ex} is expressed as a function of the acid and base catalytic rates k_a and k_b, respectively, modulated by the pH of the solvent. k_w refers to the catalytic rate of the non-dissociated water which is pH independent by definition.

The rates at which amide protons are exchanged with water vary over many orders of magnitude (Dempsey 2001). A variety of NMR methods for the determination of amide hydrogen exchange rates for proteins in solution has been developed in the past (Chevelkov et al. 2010; Jensen et al. 2007; Mori et al. 1997; Gemmecker et al. 1993; Bracken and Baum 1993). So called "non-equilibrium measurements" are performed by consecutive recording of 2D ^{1}H,^{15}N correlation experiments after addition of D_2O to the protein solution. The time decay of the signals is then fitted considering a monoexponential behavior from which the exchange rates are obtained (Wagner and Wuthrich 1982). It is obvious that the kinetic range accessible by this technique is limited by the time required for recording the spectra and sample handling. Under ideal conditions, the two-dimensional ^{1}H,^{15}N correlation spectra can be measured on the timescale of a few minutes (Andrec et al. 1995; Kay et al. 1992).

In order to access larger exchange rates, editing methods are used (Zhou and van Zijl 2006; Wojcik et al. 1999; Hwang et al. 1998; Dalvit and Hommel 1995). For example, in the MEXICO sequence (Gemmecker et al. 1993), isotope filters are employed to remove observable magnetization from all protons attached to ^{15}N and ^{13}C while water magnetization is preserved. The amide protons recover magnetization by exchange with solvent water during a mixing period. The timescale accessible by this method ranges from ca 0.2 and 20 s^{-1}, limited on one side by the longitudinal relaxation rates of the nitrogens and on the other hand by the loss of cross peak intensities in ^{1}H,^{15}N INEPT correlation spectra when the amide exchange rate approaches $^1J_{HN}$ (Forsen and Hoffman 1964). This last effect is exploited in lineshape analyses to expand the accessible window of exchange rates to $\sim$200 s^{-1} (Henry and Sykes 1993). It is interesting to note the gap between the upper limit of exchange rates accessible by the equilibrium method ($\sim$0.002 s^{-1}), and the lower limit accessible by editing methods or lineshape analysis ($\sim$0.2 s^{-1}). In the present work, we show that this gap can be filled at least partially by solid-state NMR measurements given the long ^{15}N relaxation time there, as discussed below.

It is generally accepted that proteins are undergoing motion even in the solid-state (McDermott 2009; Chevelkov et al. 2009; Hologne et al. 2006b; Giraud et al. 2004; Palmer et al. 1996; Cole and Torchia 1991). Dynamics results in disruption of hydrogen bonds, and in turn in hydrogen exchange, even for buried amides far from the polar surface of the protein. This was originally demonstrated by neutron diffraction studies, in which H/D exchange is induced by soaking the crystals in D_2O for large periods of time (weeks to years), in order to reduce the background noise from incoherent neutron scattering generated by hydrogen atoms (Wlodawer and Sjolin 1982).

H/D exchange rates in solid protein samples have been determined in the past by NMR using exchange trapping methods (Hoshino et al. 2007; Whittemore et al. 2005; Gallagher et al. 1992). In these experiments, amide exchange is allowed to occur for a specific time. Thereafter, exchange is quenched by transferring the sample into a buffer which prevents further exchange. At the same time, the solid protein is solubilized and high resolution NMR spectra can be recorded. This technique is based on non–equilibrium conditions, and the measured characteristic exchange times can not be shorter than seconds due to the time required for sample handling. Hydroxyl side chain exchange rates are much faster and can be quantified in the solid-state using EXSY type experiments (Agarwal et al. 2010). In principle, one might expect different exchange rates in solution and in the solid-state. This difference would be due to the presence of crystal contacts in the solid-state which might directly affect the internal fluctuations of the protein, and which would allow water and ions to come into contact with amides buried in the interior of the protein. This was in fact experimentally observed for BPTI (Gallagher et al. 1992) and lysozyme (Pedersen et al. 1991). In general, lower HDX rates and a considerable variation for different amide groups was observed in the solid-state. These differences, however, did not correlate in a simple manner to the presence or absence of a crystal contact for a given amide hydrogen.

The in-situ quantification of exchange rates in the solid-state, i.e. without solubilising the sample prior to the measurement, is complicated due to the presence of homogeneous interactions which are not averaged out by fast molecular tumbling. Resolution of ^{1}H resonances is poor and the detection of chemical shift isotope effects (Ottiger and Bax 1997) is impractical even at very high MAS rotation

frequencies. In this work, we show that this problem can be efficiently overcome by extensive deuteration of the protein (Akbey et al. 2010; Agarwal and Reif 2008; Chevelkov et al. 2006; Hologne et al. 2006a). We describe a new experiment for the quantification of exchange rates in the solid-state based on proton detection under equilibrium conditions. An important motivation for the present study is the quantification of the systematic errors induced by H/D exchange in the quantification of ^{15}N longitudinal relaxation rates measured previously for the α-spectrin SH3 domain (Chevelkov et al. 2008a). We observed large variations of the ^{15}N-T_1 relaxation times ranging from 1 s to more than 50 s. Given the fact that ^{15}N T_1 relaxation times were field dependent, we did not expect HDX to be dominating the relaxation times as chemical exchange is field independent. Nevertheless, its presence could not be completely ruled out, and knowledge of the exchange contribution to ^{15}N T_1 is fundamental for a correct quantification of backbone dynamics (Chevelkov et al. 2009).

Materials and methods

We used a perdeuterated sample of the SH3 domain of chicken α-spectrin, which was obtained by recombinant protein expression and purified as described previously Chevelkov et al. 2007. Crystallization was induced in a buffer by a pH-shift from 3.5 to 7.5. To achieve 50% (90%) deuteration at exchangeable sites, the protein was crystallized from a buffer containing H_2O and D_2O in a ratio of 1:1 (1:9) (Akbey et al. 2010). After precipitation overnight, crystals were spun into a 3.2 mm rotor using approximately 15 mg protein. All NMR experiments were carried out on a Bruker Biospin AVANCE spectrometer operating at a ^{1}H Larmor frequency of 400 MHz, using a 3.2 mm triple-resonance probe. The MAS frequency was adjusted to 23 kHz. The acquisition time in the proton detected experiment amounted to $t_1^{max} = 44$ ms and $t_2^{max} = 70$ ms in the indirect ^{15}N and direct ^{1}H evolution period, respectively. Total experimental times varied between 4 h and 4 days depending on the mixing times used. The effective temperature was set to ~22°C. Data processing was performed using Bruker Topspin. The 2D spectra were processed using a cosine-squared apodization function.

Results

In order to quantify HDX rates, we used a series of pulse schemes that are represented in Fig. 1. Figure 1a shows a ^{15}N detected HETCOR experiment in which a mixing period (Δ) is introduced after the ^{1}H,^{15}N CP step. During the mixing time, the initial amide protons are eventually

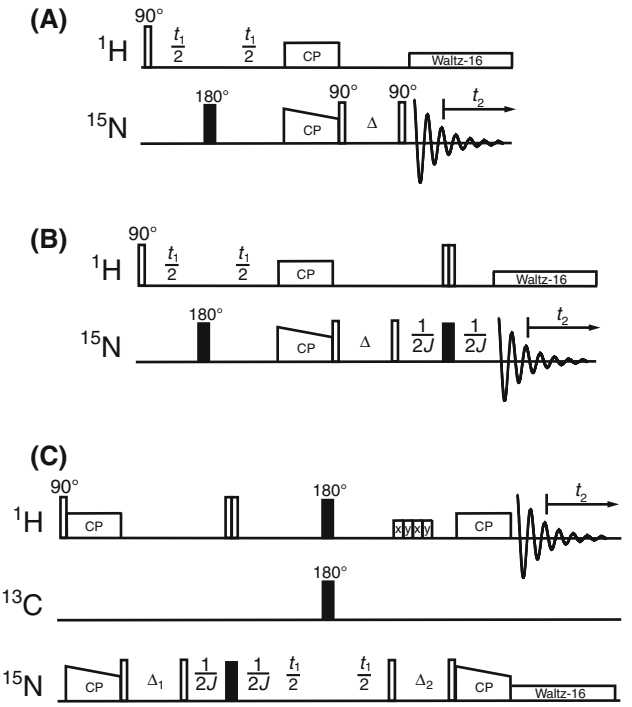

Fig. 1 Pulse schemes for the quantification of amide ^{15}N–H/D exchange rates in the solid-state. **a** ^{15}N detected ^{1}H,^{15}N correlation with a variable longitudinal mixing time Δ preceeding acquisition. HDX rates are determined by making use of ^{15}N–H/D chemical shift isotope effects which allows to separate ^{15}N–H and ^{15}N–D moities. The pulse scheme (**b**) includes a isotope filtering element which allows to discriminate between ^{15}N–D and ^{15}N–H moities prior to acquisition. **c** ^{1}H detected version of the exchange experiment. In this sequence two mixing times are employed. In the first step, chemical exchange results in a conversion from ^{15}N–H into ^{15}N–D which is selected for prior to t_1. After Δ_2 and a second chemical exchange process, magnetization is transferred back to the amide proton for detection. During the second mixing time a train of pulses is applied on the ^{1}H channel for water suppression

exchanged with deuterons of the solvent. If the time required for exchange is shorter than the individual ^{15}N longitudinal relaxation times, then a splitting between different ^{15}N chemical shifts will be observed for the amide nitrogens, which is due to chemical shift isotope effects (Benedict et al. 1996; Altman et al. 1978). Differences in ^{15}N chemical shifts between ^{15}N–H and ^{15}N–D moieties are originating from a shortening of the donor covalent bonds and a lengthening of the distance between the nitrogen atom to the acceptor upon substitution of the hydrogen by a deuteron atom. The so-called Ubbelohde effect (Ubbelohde and Gallagher 1955) is known from X-ray and neutron diffractometry and was theoretically explained by Jameson (Jameson 1991). Our experiments were inspired by a approach introduced by Chevelkov et al. 2010 for the detection of H/D exchange in solution which is a based on a (HCACO)NH-type experiment and which makes use of the deuterium isotopic effect on the nitrogen chemical shift.

Four ^{15}N detected 2D spectra were recorded using mixing times of 0.0, 0.5, 3.0 and 9.0 s. The full ^{15}N detected reference spectrum ($\Delta = 0$), as well as a ^{1}H detected ^{1}H, ^{15}N HSQC spectrum is shown as part of the supporting information (Figure S1). Most of the amide resonance frequencies remained unaffected, indicating that HDX is not significant for the majority of the amides. Exceptions are K60, S36, N35sc and Wε41, for which we observe high field shifted ^{15}N signals at increased mixing times (Fig. 2). The intensity of these signals increases from 0 at $\Delta = 0$ to a maximum value which is determined by both, the HDX rate, and the ^{15}N longitudinal relaxation time of a particular residue. At longer mixing times, the signal intensities are exponentially reduced by relaxation. The ^{15}N isotope induced chemical shift changes are 0.65 ppm for S36, 0.6 ppm for K60 and 0.4 ppm for N35sc. The isotope effect is related to the shape of the potential in which the protons are located and thus to the geometry of the hydrogen bond in which they participate (Benedict et al. 1996). This relationship has been used in the past to characterize hydrogen bond strength in peptides (Jaravine et al. 2004). For proteins in solution, a linear relation between the isotropic ^{15}N chemical shifts and the ^{15}N (H/D) chemical shift isotope effects is found experimentally. An interpretation of the values obtained here in terms of hydrogen bond strengths is out of the scope of this paper and will therefore not be discussed further. Exchange rates which exceed the frequency difference between ^{15}N–H and ^{15}N–D chemical shifts (on the order of 25 s^{-1}) would induce exchange broadening and are therefore not accessible with the presented approach.

Obviously, spectra obtained using the pulse scheme of Fig. 1a display an intrinsically low resolution, due to the doubling of the resonances in the ^{15}N dimension. Superposition of ^{15}N–H and ^{15}N–D shifts complicates a proper quantification. In order to discriminate between ^{15}N–H and ^{15}N–D moieties, we introduced the filtering element 1/(2 J_{NH}) $-90°_{x}90°_{\pm x}(^{1}H)$, $180°_{x}(^{15}N)$–1/(2 J_{NH}) (Fig. 1b) to select either ^{15}N–H or ^{15}N–D magnetization prior to t_2.

Figure 3 shows a superposition of the ^{15}N detected correlation experiments recorded using the pulse scheme of Fig. 1b with selection of ^{15}N–H moieties (black) and ^{15}N–D moieties (red) prior to detection. HDX occurs only for those resonances in which exchange was previously observed using the non-edited version of the experiment.

A quantitative analysis of the exchange rates using the experiments described above is demanding due to the intrinsically long measurement times. Ideally, a series of experiments is required with mixing times ranging from 0 up to the average expected ^{15}N longitudinal relaxation time (20–40 s) to allow a quantitative analysis of the exchange rates and to extract a correction term for ^{15}N T_1 for those residues which are undergoing HDX. In general, a significant gain in sensitivity can be obtained by designing the experiment such that protons are detected in the direct dimension. In the experiment represented in Fig. 1c, ^{1}H magnetization is transferred via CP to ^{15}N using $\tau_{CP} = 160$ µs. The short CP contact time ensures selective magnetization transfer between directly bonded ^{15}N–H spin pairs. During the mixing time Δ_1, ^{15}N–H are eventually exchanged with ^{15}N–D. An isotope filter is included at this point so that only ^{15}N–D moieties evolve chemical shift in the indirect dimension. After the filter, a second mixing period Δ_2 is implemented in which the ^{15}N–D can exchange again so that protonated amides can be detected in t_2. Examples of the resulting 2D spectra are shown in Fig. 4 (red) superimposed with the reference spectrum (black). In all cases, the two mixing times were set equal in each experiment ($\Delta = \Delta_1 = \Delta_2$). Correlation peaks appearing at larger mixing times are originating from R21, S36, and K60. Additionally, cross peak buildup was observed for W41ε and for the side chain amides of N35 and N38. Figure 5 represents the integral intensities of the correlation signals as a function of the mixing time. The experimental values were fit considering single exponentials for both, the H/D exchange process and the ^{15}N T_1 decays. ^{15}N–D T_1 and ^{15}N–H T_1 relaxation was considered individually. The evolution of the ^{15}N magnetization during the first variable delay Δ_1 can be described by the differential equation (Jeener et al. 1979):

$$\frac{\mathrm{d}}{\mathrm{dt}}\begin{pmatrix} {}^{15}\mathrm{N}-\mathrm{H}(\Delta_1) \\ {}^{15}\mathrm{N}-\mathrm{D}(\Delta_1) \end{pmatrix} = \begin{pmatrix} -\frac{1}{T_1^{\mathrm{NH}}} - k_{\mathrm{ex}} & k_{\mathrm{ex}} \\ k_{\mathrm{ex}} & -\frac{1}{T_1^{\mathrm{ND}}} - k_{\mathrm{ex}} \end{pmatrix} \begin{pmatrix} {}^{15}\mathrm{N}-\mathrm{H}(\Delta_1) \\ {}^{15}\mathrm{N}-\mathrm{D}(\Delta_1) \end{pmatrix} \tag{3}$$

Solving Eq. 3 for $^{15}\mathrm{N}-\mathrm{D}(\Delta_1)$we obtain

$$^{15}N - D(\Delta_1) = -\frac{\left(e\left(\frac{\Delta_1(-T_1^{\mathrm{ND}}-T_1^{\mathrm{NH}}-2T_1^{\mathrm{ND}}T_1^{\mathrm{NH}}k_{\mathrm{ex}}-B)}{2T_1^{\mathrm{ND}}T_1^{\mathrm{NH}}}\right) - e\left(\frac{\Delta_1(-T_1^{\mathrm{ND}}-T_1^{\mathrm{NH}}-2T_1^{\mathrm{ND}}T_1^{\mathrm{NH}}k_{\mathrm{ex}}+B)}{2T_1^{ND}T_1^{NH}}\right)\right)}{B} T_1^{\mathrm{ND}}T_1^{\mathrm{NH}}k_{\mathrm{ex}} \tag{4}$$

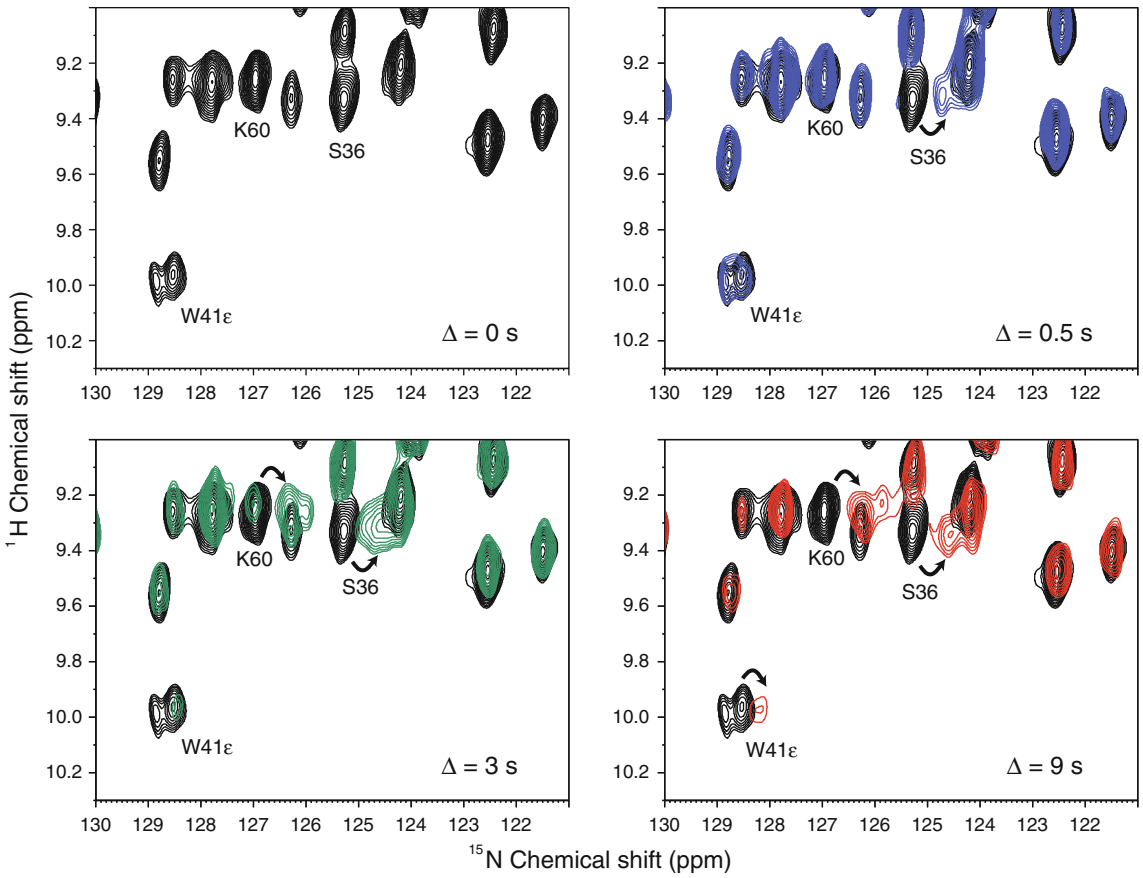

Fig. 2 ^{15}N detected ^{1}H, ^{15}N correlation spectra recorded using the pulse scheme shown in Fig. 1a, using mixing times $\Delta = 0.0$ s (*black*) and 0.5 s (*blue*), 3.0 (*green*) and 9.0 s (*red*). Residues in which HDX occurs during the mixing time appear upfield shited in the ^{15}N dimension due to the deuterium isotope effect. Residues showing exchange are indicated by *arrows*. The experiments were recorded using a perdeuterated SH3 sample which contained 10% protons at exchangeable sites

where

$$B = \sqrt{\left(T_1^{ND}\right)^2 - 2T_1^{ND}T_1^{NH} + \left(T_1^{NH}\right)^2 + 4(k_{ex})^2\left(T_1^{ND}\right)^2\left(T_1^{NH}\right)^2} \tag{5}$$

Equation 4 describes the amount of ^{15}N–D(Δ_1) magnetization created during the first mixing period. During the second mixing time, the magnetization ^{15}N–D(Δ_1) is eventually reconverted into ^{15}N–H due to a second exchange process. At the end of this second mixing period, protons are detected and consequently all residual ^{15}N–D(Δ_2) magnetization is discarded. Re-iterating the differential equation (Eq. 3) by using Eq. 4, yields the following expression for the amount of ^{15}N–H(Δ_2) magnetization as a function of T_1^{NH}, T_1^{ND}, k_{ex} and the mixing times Δ_1 and Δ_2, prior to the CP back-transfer step

where A is a constant introduced for scaling of the curve (A = 1 represents the case where the fitted data are normalized to a maximum intensity of 1 etc.).

The best fit of the experimental data is represented by the solid lines in Fig. 5. The fit parameters are listed in Table 1. The upper and lower dashed lines correspond to the predicted values for the signal intensities, assuming $T_1^{ND} = \infty$ and $T_1^{ND} = T_1^{NH}$, respectively. Apparently, the uncertainty in the fit of T_1^{ND} matches approximately the error bars of the experimental data (noise RMSD). Accurate values for longitudinal relaxation times could not be determined. On the other hand, all the information concerning the H/D exchange rates is included in the initial buildup rates, which are not influenced by the longitudinal relaxation in case those are sufficiently long in comparison to the exchange rates. The experimental

$$^{15}\mathrm{N} - D(\Delta_2) = -A\frac{\left(e\left(\frac{\Delta_2(-T_1^{ND}-T_1^{NH}-2T_1^{ND}T_1^{NH}k_{ex}-B)}{2T_1^{ND}T_1^{NH}}\right) - e\left(\frac{\Delta_2(-T_1^{ND}-T_1^{NH}-2T_1^{ND}T_1^{NH}k_{ex}+B)}{2T_1^{ND}T_1^{NH}}\right)\right)}{B} T_1^{ND}T_1^{NH}k_{ex}{}^{15}\mathrm{N} - \mathrm{D}(\Delta_1) \tag{6}$$

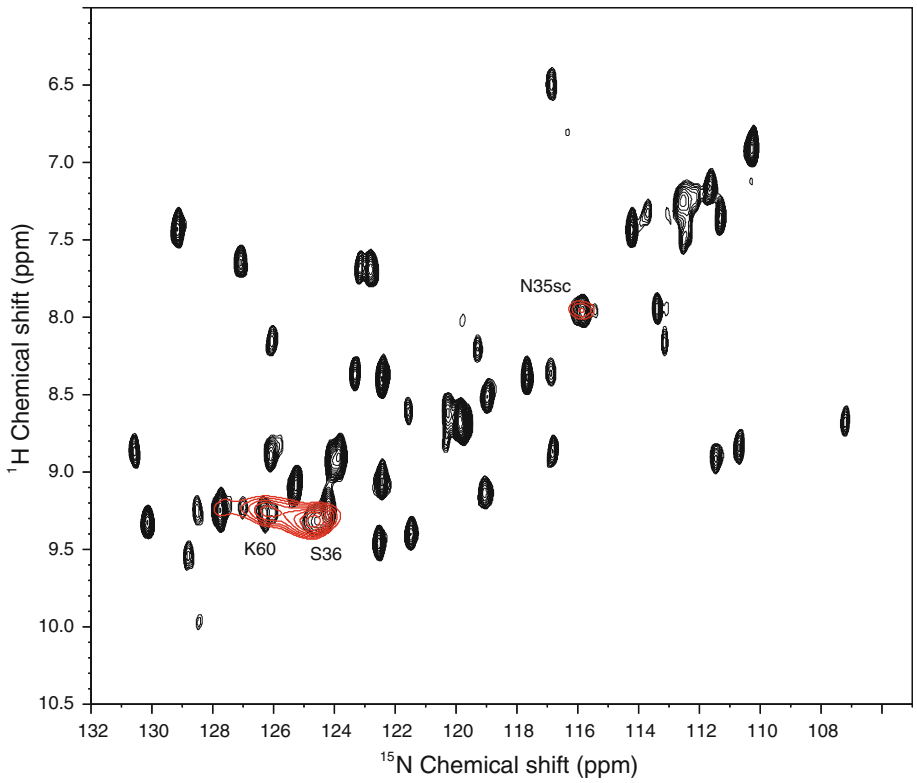

Fig. 3 ^{15}N detected ^{1}H, ^{15}N correlation spectrum recorded using the pulse scheme shown in Fig, 1b. In the *black* spectrum, ^{15}N–H magnetization was selected prior to detection ($\Delta = 3.0$ s), while for the red spectrum ^{15}N–D were allowed to pass through the filter ($\Delta = 3.0$ s). HDX is observed for residues S38, K60 and the sidechain amides of N35. The ^{15}N–D correlations are up-field shifted due to the H/D isotope effect on the ^{15}N chemical shift. The experiments were recorded using a perdeuterated SH3 sample which contained 10% protons at exchangeable sites

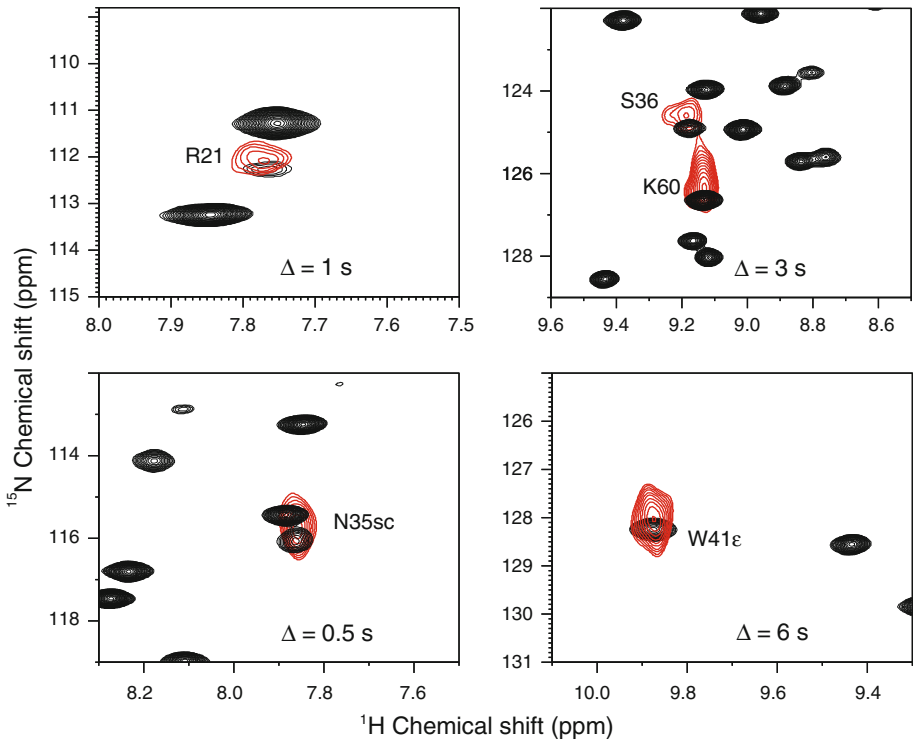

Fig. 4 Representative ^{1}H,^{15}N correlation spectra employing the ^{1}H detected, isotope edited, double exchange pulse scheme shown in Fig. 1c (*red contour lines*). In the ^{15}N dimension, resonances are up-field shifted due to the H/D isotope effect. The INEPT based HSQC reference spectrum is represented in *black*. In the exchange experiment, the two mixing times were set equal in each experiment ($\Delta = \Delta_1 = \Delta_2$). HDX was observed for residues R21, S36 and K60, as well as for the sidechains of N35, N38 and W41. The experiments were recorded using a perdeuterated SH3 sample which contained 50% protons at exchangeable sites

values in Fig. 6 were normalized to the intensities calculated at infinite mixing times in absence of ^{15}N relaxation as shown in Fig. 5 for K60 as an example.

The cross peaks intensities obtained by integration of the spectra, were initially plotted as a function of the mixing time (Δ) in arbitrary units using Eq. 6 (Fig. 5). The value of A obtained from this fitting is used for normalization of the experimental values. Thus, a value of 1 in Fig. 6, refers to the case in which the H/D populations are completely equilibrated by chemical

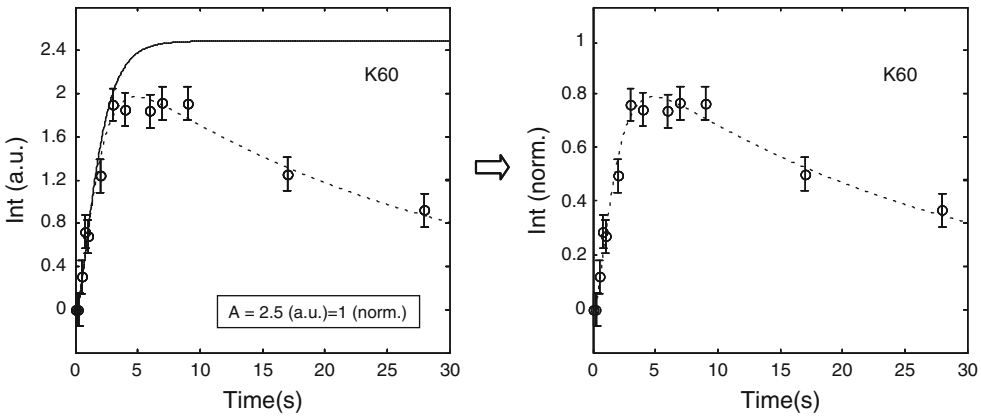

Fig. 5 The method used for data normalization is exemplified with the values obtained for K60. For more information see text

Table 1 Best fit H/D exchange rates k_{ex}, T_1(ND) and T_1(NH) relaxation times for residues undergoing H/D chemical exchange in the α-spectrin SH3 domain

	K60	S36	R21	W41ε	N35sc	N38sc
T_1^{NH}(s)	40 ± 8	25 ± 10	5 ± 3	12 ± 8	20 ± 9	20 ± 10
T_1^{ND}(s)	80 ± 8	50 ± 10	10 ± 3	24 ± 8	40 ± 9	40 ± 10
k_{ex} (s^{-1})	0.38 ± 0.06	3 ± 1	2 ± 1	0.2 ± 0.1	5 ± 1	0.3 ± 0.1

The fit was obtained using Eq. 6

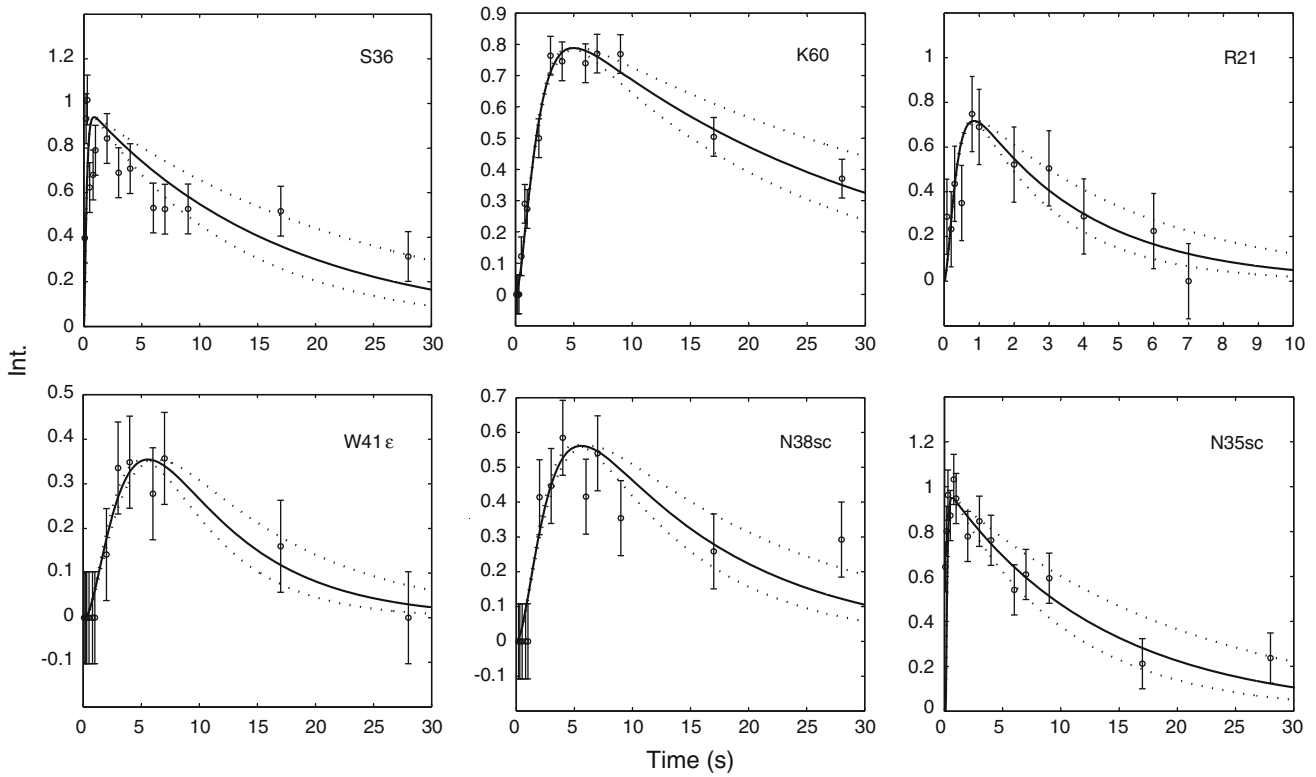

Fig. 6 Experimental and theoretical intensities for residues undergoing H/D exchange as a function of the exchange mixing times Δ. The buildup and decay curves were fitted using Eq. 6 (*solid lines*). Fit parameters are listed in Table 1. The *lower dashed lines* assume T_1(ND) = T_1(NH), whereas T_1(ND) = ∞ for the *upper dashed ones*

exchange, while at the same time ^{15}N longitudinal relaxation did not affect the magnetization yet. For longer mixing times, the intensities decay exponentially due to longitudinal relaxation. In this situation, the initial rates are independent of the ^{15}N T_1 relaxation within experimental error.

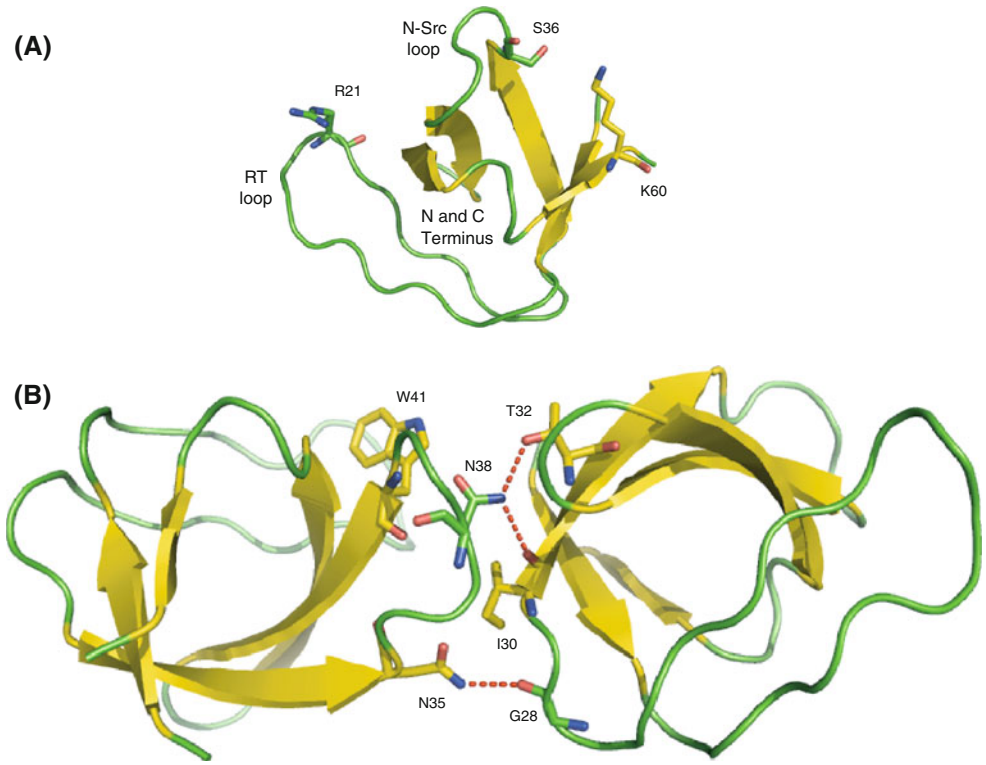

Fig. 7 Crystal structure of the α-spectrin SH3 domain (PDB code: 1U06, Chevelkov et al. 2005). **a** Residues which are subject to backbone H/D chemcial exchange are represented by *sticks*. b Crystal contacts between symmetry related SH3 molecules involving the n-Src loop

Discussion

We demonstrated that H/D exchange rates of backbone amide protons in proteins are accessible by MAS solid-state NMR. The experiments were carried out using a microcrystalline sample of the α-spectrin SH3 domain. We observed chemical exchange for 6 residues with H/D exchange rates in the range from 0.2 to 5 s^{-1}. For all other amides, no H/D exchange could be observed. This implies that H/D exchange does not play a significant role for most residues in the α-spectrin SH3 domain within their characteristic ^{15}N longitudinal relaxation times. The analysis of dynamics in the solid-state that we have reported earlier (Chevelkov et al. 2009) seems thus not systematically affected by H/D exchange, and large fluctuations of the ^{15}N T_1 relaxation times reported previously (Chevelkov et al. 2008a) are in fact originating from local dynamics. The residues for which we could quantify H/D exchange rates (Table 1) have typically long ^{15}N relaxation times. We could not characterize chemical exchange rates for residues located in highly flexible regions of the protein, like the C-terminal D62. This is due to the fact that ^{15}N longitudinal relaxation times are very short for those residues, which is a consequence of large amplitude motions. In fact, we observe dramatically reduced CP efficiencies in certain loop regions, as well as at the N-terminus and the C-terminus of the protein (Linser et al. 2010). TROSY type experiments turned out to be essential to assign these regions of the protein. In order to quantitatively access the H/D exchange properties in these parts of the protein, the experiments need to be adapted and should make use of spin-state selective coherence transfer pulse sequence elements. At this point, there is no evidence that H/D exchange plays an important role for those residues undergoing intermediate motion on a ns-μs timescale motion.

Figure 7a highlights residues for which we observe backbone chemical exchange using the structure of the α-spectrin SH3 domain (PDB: 1U06). We find chemical exchange in particular for residues S36, N35 and N38 which are part of the n-Src loop. This region seems in fact to be flexible. The amides resonances of S36, N35, N38 are only visible at lower temperature and disappear at an effective temperature of 22°C (Linser et al. 2010). In INEPT type experiments, S36, N35, N38 display decreased intensities in comparison to CP experiments, which indicates that the n-Src loop undergoes chemical exchange and can adopt multiple conformations. This is confirmed in CODEX experiments which probe motion on a millisecond timescale (Krushelnitsky et al. 2009). K60 is located at the

edge of the last β-sheet, and R21 at the tip of the extended RT-loop. For these two residues an increased mobility might be expected.

In Fig. 7b, the sidechains of residues N35, N38 and W41 are shown in a stick representation together with the interacting residues in the symmetry related molecule. The sidechain of N38, located in the N-Src-loop, is within hydrogen bonding distance to both T32-OH and the carbonyl group of I30 in a symmetry related molecule. This might explain a restricted mobility of this group, and thus an increased ^{15}N–T_1 relaxation time. For a similar reason, the sidechain of N35 might show detectable H/D chemical exchange rates, as N35 is involved in an intermolecular hydrogen bond to the carbonyl group of G28.

To conclude, we could demonstrate that backbone H/D exchange rates are accessible in the solid-state in a direct correlation experiment. We find that H/D exchange rates are not significant for rigid residues located in regular secondary structure elements. Thus, ^{15}N-T_1 relaxation times are not compromised in a motional analysis. We observe the largest H/D exchange rates (2–5 s^{-1}) for the n-Src loop in α-spectrin SH3 which was shown before to undergo conformational exchange.

Acknowledgments J.M.L is a DFG postdoctoral scholar and acknowledges financial support from the DFG. This research was supported by the Leibniz-Gemeinschaft and the DFG (Re1435, SFB449, SFB740).

References

Agarwal V, Reif B (2008) Residual methyl protonation in perdeuterated proteins for multi-dimensional correlation experiments in MAS solid-state NMR spectroscopy. J Magn Reson 194:16–24

Agarwal V, Linser R, Fink U, Faelber K, Reif B (2010) Identification of hydroxyl protons, determination of their exchange dynamics, and characterization of hydrogen bonding in a Microcrystallin protein. J Am Chem Soc 132:3187–3195

Akbey U, Lange S, TrentFranks W, Linser R, Rehbein K, Diehl A, van Rossum BJ, Reif B, Oschkinat H (2010) Optimum levels of exchangeable protons in perdeuterated proteins for proton detection in MAS solid-state NMR spectroscopy. J Biomol NMR 46:67–73

Altman LJ, Laungani D, Gunnarsson G, Wennerstrom H, Forsen S (1978) Proton, deuterium, and tritium nuclear magnetic-resonance of intra-molecular hydrogen-bonds—isotope effects and shape of potential-energy function. J Am Chem Soc 100:8264–8266

Andrec M, Hill RB, Prestegard JH (1995) Amide exchange-rates in escherichia-coli acyl carrier protein—correlation with protein-structure and dynamics. Prot Science 4:983–993

Bai YW, Sosnick TR, Mayne L, Englander SW (1995) Protein-folding intermediates—native-state hydrogen-exchange. Science 269:192–197

Benedict H, Hoelger C, AguilarParrilla F, Fehlhammer WP, Wehlan M, Janoschek R, Limbach HH (1996) Hydrogen/deuterium isotope effects on the N-15 NMR chemical shifts and geometries of low-barrier hydrogen bonds in the solid state. J Molec Struct 378:11–16

Bracken C, Baum J (1993) Determination of amide exchange-rates by measurement of 2d nmr line-broadening. J Am Chem Soc 115:6346–6348

Chevelkov V, Faelber K, Diehl A, Heinemann U, Oschkinat H, Reif B (2005) Detection of dynamic water molecules in a microcrystalline sample of the SH3 domain of a-spectrin by MAS solid-state NMR. J Biomol NMR 31:295–310

Chevelkov V, Rehbein K, Diehl A, Reif B (2006) Ultrahigh resolution in proton solid-state NMR spectroscopy at high levels of deuteration. Angewandte Chemie-International Edition 45: 3878–3881

Chevelkov V, Faelber K, Schrey A, Rehbein K, Diehl A, Reif B (2007) Differential line broadening in MAS solid-state NMR due to dynamic interference. J Am Chem Soc 129:10195–10200

Chevelkov V, Diehl A, Reif B (2008a) Measurement of 15 N–T1 relaxation rates in a perdeuterated protein by magic angle spinning solid-state nuclear magnetic resonance spectroscopy. J Chem Phys 128:052316

Chevelkov V, Diehl A and Reif B (2008b) Measurement of N-15-T-1 relaxation rates in a perdeuterated protein by magic angle spinning solid-state nuclear magnetic resonance spectroscopy. J Chem Phys 128

Chevelkov V, Fink U, Reif B (2009) Quantitative analysis of backbone motion in proteins using MAS solid-state NMR spectroscopy. J Biomol NMR 45:197–206

Chevelkov V, Xue Y, Rao DK, Forman-Kay JD, Skrynnikov NR (2010) 15NH/D-SOLEXSY experiment for accurate measurement of amide solvent exchange rates: application to denatured drkN SH3. J Biomol NMR 46:227–244

Cole HBR, Torchia DA (1991) An NMR study of the backbone dynamics of staphylococcal nuclease in the crystalline state. Chem Physics 158:271–281

Dalvit C, Hommel U (1995) Sensitivity-improved detection of protein hydration and its extension to the assignment of fast-exchanging resonances. J Magn Reson B 109:334–338

Dempsey CE (2001) Hydrogen exchange in peptides and proteins using NMR-spectroscopy. Prog Nucl Magn Reson Spectrosc 39:135–170

Dyson HJ, Kostic M, Liu J, Martinez-Yamout MA (2008) Hydrogen-deuterium exchange strategy for delineation of contact sites in protein complexes. Febs Letters 582:1495–1500

Forsen S, Hoffman RA (1964) Exchange rates by nuclear magnetic multiple resonance. 3. Exchange reactions in systems with several nonequivalent sites. J Chem Phys 40:1189–1190

Gallagher W, Tao F, Woodward C (1992) Comparison of hydrogen-exchange rates for bovine pancreatic trypsin-inhibitor in crystals and in solution. Biochemistry 31:4673–4680

Gemmecker G, Jahnke W, Kessler H (1993) Measurement of fast proton-exchange rates in isotopically labeled compounds. J Am Chem Soc 115:11620–11621

Giraud N, Bockmann A, Lesage A, Penin F, Blackledge M, Emsley L (2004) Site-specific backbone dynamics from a crystalline protein by solid-state NMR spectroscopy. J Am Chem Soc 126:11422–11423

Gregory RB, Crabo L, Percy AJ, Rosenberg A (1983) Water catalysis of peptide hydrogen isotope exchange. Biochemistry 22:910–917

Halskau O, Froystein NA, Muga A, Martinez A (2002) The membrane-bound conformation of alpha-lactalbumin studied by NMR-monitored H-1 exchange. J Mol Biol 321:99–110

Henry GD, Sykes BD (1993) Saturation-transfer of exchangeable protons in H-1-decoupled N-15 inept spectra in water—application to the measurement of hydrogen-exchange rates in amides and proteins. J Magn Reson B 102:193–200

Hologne M, Chen ZJ, Reif B (2006a) Characterization of dynamic processes using deuterium in uniformly H-2, C-13, N-15

enriched peptides by MAS solid-state NMR. J Magn Reson 179:20–28

Hologne M, Chevelkov V, Reif B (2006b) Deuterated peptides and proteins in MAS solid-state NMR. Prog Nucl Magn Reson Spectrosc 48:211–232

Hoshino M, Katou H, Yamaguchi KI, Goto Y (2007) Dimethylsulfoxide-quenched hydrogen/deuterium exchange method to study amyloid fibril structure. Biochimica Et Biophysica Acta-Biomembranes 1768:1886–1899

Hvidt A, Nielsen SO (1966) Hydrogen exchange in protein insulin, ribonuclease, beta -lactoglobulin, myoglobin, chymotryp-sinogen, yeast alcohol dehydrogenase collagen, bovine serum albumin. Advance Protein Chem 21:287–386

Hwang TL, van Zijl PCM, Mori S (1998) Accurate quantitation of water-amide proton exchange rates using the Phase-Modulated CLEAN chemical EXchange (CLEANEX-PM) approach with a Fast-HSQC (FHSQC) detection scheme. J Biomol NMR 11:221–226

Jameson CJ (1991) The dynamic and electronic factors in isotope effects on NMR parameters. In: Buncel E, Jones JR (eds) Isotopes in the physical and biomedical sciences, vol 2. Elsevier, Amsterdam, pp 1–54

Jaravine VA, Cordier F, Grzesiek S (2004) Quantification of H/D isotope effects on protein hydrogen-bonds by (h3)J(NC ‘) and (1)J(NC ‘) couplings and peptide group N-15 and C-13 ‘ chemical shifts. J Biomol NMR 29:309–318

Jeener J, Meier BH, Bachmann P, Ernst RR (1979) Investigation of exchange processes by 2-dimensional Nmr-spectroscopy. J Chem Physics 71:4546–4553

Jensen MR, Kristensen SM, Led JJ (2007) Elimination of spin diffusion effects in saturation transfer experiments: application to hydrogen exchange in proteins. Magn Reson Chem 45: 257–261

Kato H, Gruschus J, Ghirlando R, Tjandra N, Bai YW (2009) Characterization of the N-terminal tail domain of histone H3 in condensed nucleosome arrays by hydrogen exchange and NMR. J Am Chem Soc 131:15104–15105

Kay LE, Keifer P, Saarinen T (1992) Pure absorption gradient enhanced heteronuclear single quantum correlation spectroscopy with improved sensitivity. J Am Chem Soc 114:10663–10665

Krushelnitsky A, de Azevedo E, Linser R, Reif B, Saalwächter K, Reichert D (2009) Direct observation of millisecond to second motions in proteins by dipolar CODEX NMR. J Am Chem Soc 131:12097–12099

Kuroda Y, Endo S, Nagayama K, Wada A (1995) Stability of alpha-helices in a Molten Globule State of Cytochrome-C by hydrogen-deuterium exchange and 2-dimensional Nmr-spectroscopy. J Mol Biol 247:682–688

Linser R, Fink U, Reif B (2010) Assignment of dynamic regions in biological solids enabled by spin-selective NMR experiments. J Am Chem Soc 132:8891–8893

Maity H, Lim WK, Rumbley JN, Englander SW (2003) Protein hydrogen exchange mechanism: local fluctuations. Protein Sci 12:153–160

McDermott A (2009) Structure and dynamics of membrane proteins by magic angle spinning solid-state NMR. Ann Rev Biophys 38:385–403

Mori S, van Zijl PCM, Shortle D (1997) Measurement of water-amide proton exchange rates in the denatured state of staphylococcal nuclease by a magnetization transfer technique. Proteins-Structure Funct Genet 28:325–332

Ottiger M, Bax A (1997) An empirical correlation between amide deuterium isotope effects on C-13(alpha) chemical shifts and protein backbone conformation. J Am Chem Soc 119:8070–8075

Palmer AG, Williams J, McDermott A (1996) Nuclear magnetic resonance studies of biopolymer dynamics. J Phys Chem 100:13293–13310

Parker MJ, Marqusee S (2000) A statistical appraisal of native state hydrogen exchange data: evidence for a burst phase continuum? J Mol Biol 300:1361–1375

Pedersen TG, Sigurskjold BW, Andersen KV, Kjaer M, Poulsen FM, Dobson CM, Redfield C (1991) A nuclear-magnetic-resonance study of the hydrogen-exchange behavior of lysozyme in crystals and solution. J Mol Biol 218:413–426

Pinheiro TJT, Cheng H, Seeholzer SH, Roder H (2000) Direct evidence for the cooperative unfolding of cytochrome c in lipid membranes from H-H-2 exchange kinetics. J Mol Biol 303:617–626

Polshakov VI, Birdsall B, Feeney J (2006) Effects of co-operative ligand binding on protein amide NH hydrogen exchange. J Mol Biol 356:886–903

Raschke TM, Marqusee S (1998) Hydrogen exchange studies of protein structure. Curr Opin Biotechnol 9:80–86

Truhlar SME, Croy CH, Torpey JW, Koeppe JR, Komives EA (2006) Solvent accessibility of protein surfaces by amide H/H-2 exchange MALDI-TOF mass spectrometry. J Am Chem Soc Mass Spect 17:1490–1497

Ubbelohde AR, Gallagher KJ (1955) Acid-base effects in hydrogen bonds in crystals. Acta Crystallogr A 8:71–83

Wagner G, Wuthrich K (1982) Amide proton-exchange and surface conformation of the basic pancreatic trypsin-inhibitor in solution—studies with two-dimensional nuclear magnetic-resonance. J Mol Biol 160:343–361

Whittemore NA, Mishra R, Kheterpal I, Williams AD, Wetzel R, Serpersu EH (2005) Hydrogen-deuterium (H/D) exchange mapping of Aβ1–40 amyloid fibril secondary structure using nuclear magnetic resonance spectroscopy. Biochemistry 44:4434–4441

Wlodawer A, Sjolin L (1982) Hydrogen-exchange in Rnase a—neutron-diffraction study. Proceedings of the National Academy of Sciences of the United States of America-Biological Sciences 79:1418–1422

Wojcik J, Ruszczynska K, Zhukov I, Ejchart A (1999) NMR measurements of proton exchange between solvent and peptides and proteins. Acta Biochim Pol 46:651–663

Wong PTT, Heremans K (1988) Pressure effects on protein secondary structure and hydrogen-deuterium exchange in chymotrypsinogen—a Fourier-transform infrared spectroscopic study. Biochim Biophys Acta 956:1–9

Zhou JY, van Zijl PCM (2006) Chemical exchange saturation transfer imaging and spectroscopy. Prog Nucl Magn Reson Spectrosc 48:109–136